

Y su vista solamente alcanzaba aquel lugar donde estaba y no se daba cuenta que su mirada no abarcaba todo el mundo.

Versículo 92. **Popol Vuh.**

Chapter 3

A quantitative comparison of methodologies for classifying burned areas with LISS-III imagery, and their partial contribution in the frame of a tree decision classifier.

Abstract

Large forest fires are becoming more frequent in Mediterranean areas due to climatic factors and changes in lifestyles and socioeconomic conditions. It is important therefore, to dispose of techniques to efficiently evaluate fire effects in burned areas. There is a long list of potential methodologies to survey burned areas, but little effort has been done to establish quantitative comparisons among these techniques to determine the most accurate one. To address this deficiency, this study will quantitatively evaluate the accuracy of five different techniques: a field survey and four satellite-based techniques (spectral unmixing, vegetation indexes, texture and raw reflectance data), in order to classify a large forest fire occurred in 1994 in Solsonès (NE Spain). Three pure classes were determined by means of a Maximum Likelihood classifier: burned area, unburned vegetation, and soil; and a non-pure class: mixed area. As a further step, classified images obtained by each methodologies were included into a tree classifier, to investigate their partial contribution to the classification process. When pure classes were considered, the most accurate methodologies were: Reflectance Data and Spectral Unmixing (82% of overall accuracy), versus the poorer performances of Vegetation Indices (70%), Textural measures (72%) and the Field Survey (68.6%). Since no image processing technique was applied to the Raw Reflectance Data, it can be considered the most cost-effective methodology, and its importance was reinforced by the tree classifier. Among the Reflectance bands, Short Wave Infrared (SWIR) and Near Infrared bands play major roles in determining the final classification of burned areas. When both pure and non-pure classes were considered, overall accuracy decreased around 30-40%, depending on the method, offering an unacceptably low accuracy. Further discussion is offered about the limitations of each technique and the sources of noise that influenced final accuracy values, grouped into pre-classification, classification, and post-classification steps. The results of this study reveal that time consuming and expensive methods are not necessarily the most accurate, especially when potentially easily distinguishable classes are involved.

Keywords: fire; Mediterranean areas; texture; spectral unmixing; reflectance data; vegetation indices; field survey;

INTRODUCTION

The importance of monitoring fire activity has long been recognized due to its influence on the structure and functioning of terrestrial ecosystems, as well as on global climate (Crutzen & Goldammer 1993; Levine et al., 1995). In the last decades, efforts have focused on developing methodologies capable of producing more accurate burned area estimates (Justice et al., 1993), and to improve the efficiency of remote sensing techniques to evaluate the economical, ecological and climatic effects of forest fires (Kaufman et al., 1992, Martín et al. 1999, Giglio & Kendall 2001). Among the classical remote sensing techniques, satellite imagery has been considered to offer significant advantages over conventional fire detection, monitoring and mapping methods -mainly field surveys and aerial photography- (Martín et al., 1999). Advantages of spaceborne data include the varied temporal, spatial and spectral resolutions of these instruments (Justice et al., 1993); the effectiveness of the cost/benefit ratio, especially in cases of large geographic extent (Lauer & Krumpal 1973 *in* Caetano 1995); the speed and objectivity of data processing due to its digital data format (Caetano et al., 1994); and a timely and methodologically consistent manner of gathering the required data (Pereira et al., 1999).

In spite of these advantages, satellite imagery is not free of errors, which are mainly conditioned by the goal of the study (Koutsias et al., 1999), and by more technical aspects, such as the spectral properties used by the sensor to detect and characterize the land cover of interest (Robinson 1991). When the goal of the research focuses on short term post-fire assessment, the spectral properties of the ashes are used (Robinson 1991, Pereira et al., 1999). However, the discrimination ability of the sensor to detect and characterize these burned areas will be influenced by the spectral contrast among the burned vegetation and the original background (Robinson 1991, Razafimanilo et al., 1995). A lack of spectral contrast is partly responsible for the classical errors related to post-fire classifications of burned areas (see review in Koutsias et al., 1999): i) confusion of burned areas with dark land covers (water, dark forests), ii) confusion between slightly burned and sparsely unburned vegetation (problem of the mixed pixels), iii) difficulties in discriminating burned severities and types of damage (trunk damage, surface damage, crown damage), and iv) confusion between burned vegetation and non vegetated categories, such as urban areas. In the case of Mediterranean vegetation, fire damage assessment is additionally complicated by the complex spatial patterns of its landscape (Koutsias et al., 1999), as well as a variety of phenological responses in time and space (Salvador & Pons 1996). These remote sensing problems are also related to limitations of the radiance reception (Richards 1994), such as atmospheric and topographic characteristics; sensor acquisition limitations, such as the view angle, solar zenith; and spectral, spatial and temporal resolution limitations (Caetano 1995). To minimize these problems, it has usually been necessary to combine diverse remote sensing systems and a variety of image processing techniques (Justice et al., 1993).

Among the large number of techniques applied for the characterization of burned areas (see review in Chuvieco 1999), only a few have quantitatively compared their accuracies (Chuvieco & Congalton 1988; Koutsias et al. 1999), offering little information about the potential and limitations of each technique. To address this issue, this study focuses on a quantitative comparison of five different methodologies for

mapping burned area using a case study of a large forest fire that burned in north-eastern Spain, in 1998. Strength has been given to the techniques and not to the classification algorithms, exclusively relying on the Maximum Likelihood algorithm. The selected techniques included a field survey (FS) and three broad categories of image processing, Spectral Mixing Analysis (SMA), ratio-based Vegetation Indices (VI) and image texture. Within the latter two categories, several different vegetation indices and textural measures were calculated. Performance was also evaluated using the original bands corrected to apparent surface reflectance. This fifth technique will be designated as "Raw Reflectance Data". Regarding the potentials of these five selected techniques, Field Surveys are time-consuming and expensive methodologies that tend to have high classification accuracy but lack spatial detail, with accuracy diminished by a diversity of factors (Martin et al., 1999, Rodríguez-Silva et al., 1997). In contrast, satellite based techniques provide improved fine-scale mapping and potentially more quantitative results, but they are constrained by their own set of limitations. These limitations refer to the way these techniques operate with the spectral responses of the pixels, to extract information of the ecological variable of interest. In the case of post-fire assessment, the potential of Spectral Mixing Analysis relies on the sub-pixel analysis of the materials of a burned area. This allows to quantify the relative amount of burned and unburned vegetation, and to apply direct land management measures (Caetano et al., 1994, 1996). For these characteristics, this technique has been reported to cope better with the problem of the mixed pixel (Caetano et al., 1994), and it is also likely to improve the differentiation among burn severities. In the case of Vegetation Indices, their potential rely on the differential spectral response among red, near-infrared or middle-infrared bands to detect and characterize burned areas (Milne 1986, Chuvieco & Congalton 1988, Cahoon et al. 1992). Their ratio structured equations have also been reported to reduce topographic effects (Kasischke et al. 1993). These factors might help reducing confusions between dark land covers. The potential of texture analyses on burned land assessment is conditioned by the existence of areas with homogeneous tonal intensities, associated to a given burn category. This ability to exclusively relate to the distribution of tone values, could help improving the confusion among dark land covers. It could also help differentiating burn severities. For the case of the Apparent Surface Reflectance Data, its potential refer to the utility of NIR (near-Infrared) and SWIR (Shortwave Infrared) bands to characterize burned land (Pereira et al., 1999), and a wide range of values to determine differences among burned classes, not being restricted by value thresholds offered by other techniques (i.e. vegetation indices) (Lawrence & Ripple 1998).

To establish a quantitative comparison between these techniques, this study will consider three pure classes (soil, unburned class and burned land) and one non-pure class (mixed areas). Confusion matrices, and Z-statistics (Congalton 1991; Stehman 1996) were used to determine the most adequate method to categorize the burned area into the considered classes. The weight of each processing technique to separate the final classes was determined by means of a decision tree classifier. This allowed us to establish a hierarchy among the employed methodologies, and to revise their contribution in the classification process.

MATERIAL AND METHODS

STUDY AREA

The large 1998 forest fire was located in El Solsonès county, North-Eastern Spain, between 41° 59' and 41°

44' North and 1° 21' and 1° 39' East (Figure 1). Fire started in two consecutive days (18th and 19th of July) as two separate fronts. These individual fires combined into one large front (25 km), that was favoured by the synoptic climatic conditions (warm and dry wind). Fire was finally extinguished on the 21st of July, affecting a final extension of approx. 26000 hectares. Fire temperatures reached 800 °C, with maximum rates of fire spread of 12.5 km hr⁻¹, and maximum flame heights of 80 meters (González & Castellnou 1998), indicating the severity of this episode. The resulting burned land was characterized by areas of high spatial heterogeneity in the distribution of burn severities. 67% of the total burned area affected forested lands with the rest composed of agrarian crop-fields (IEFC 2000). The primary forest species affected included *Pinus nigra* (74%), *Pinus halepensis* (11%), *Quercus faginea* (7%) and *Quercus ilex* (3%) (González & Castellnou 1998). Three climatic areas can be distinguished within the burned area, with slight differences among them. 69% of the fire land is characterized by 100-200 mm of hydric deficit (Thornthwaite classification, WWW1). Annual rainfall within this area is approximately 650-700 mm, with a summer mean precipitation of 140 mm. Annual temperatures oscillate between 12°C, with mean temperatures in the month of July of 21°C (WWW1). The area is characterized by a marked topographic gradient, decreasing towards the south. Soils are mainly bright calcareous sandstones and loams.

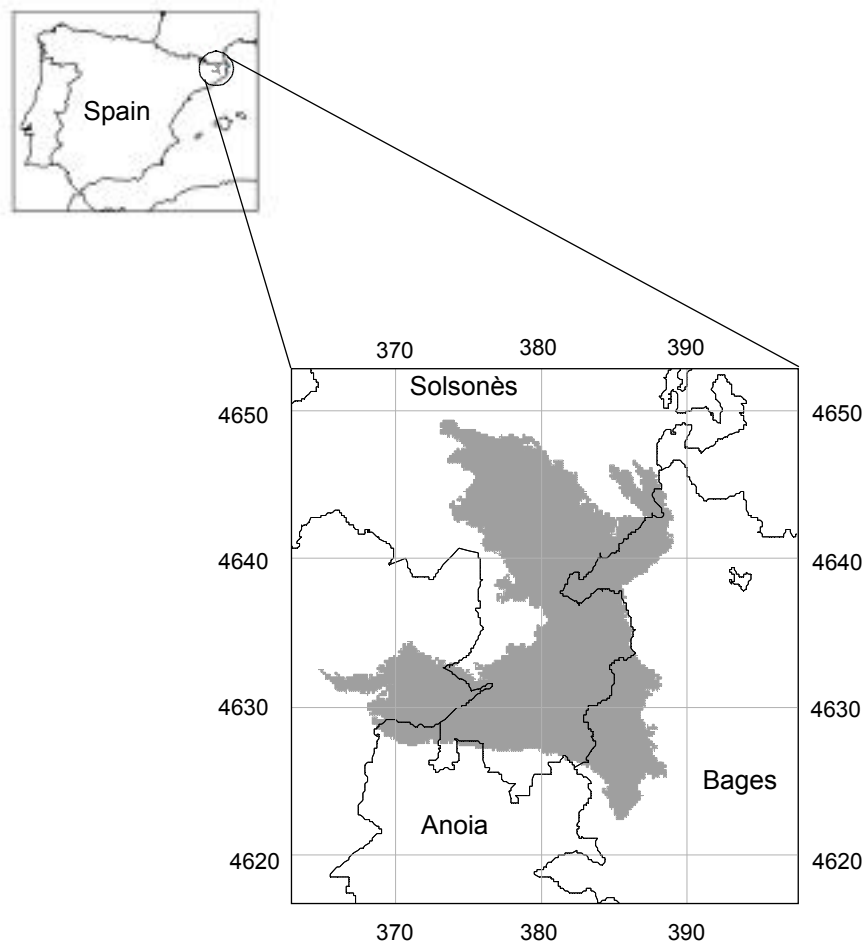


Figure 1: Location of the Solsonès 1998 large forest fire in north-eastern Spain.

Data sources

Data were obtained from three different sources: satellite images, aerial photography and a field survey:

1-Satellite imagery: An IRS-LISS III (Linear Imaging Self Scanning) post-fire image, acquired on 21 August of 1998, was used. It was a quarter of scene, path 20, row 40, covering an area of approximately 72 ×75 km. Its four bands were utilized: B2 (0.52-0.59 μm, green), B3 (0.62-0.68 μm, red), B4 (0.77-0.86 μm, near infrared), and B5 (1.55-1.70 μm, short wave infrared). The ground Instantaneous Field of View of the first three bands is 25 meters, while the fourth band had an original resolution of 70.8 m (WWW2), which was resampled to 25 m in this study. A Landsat-TM pre-fire image, acquired on 11 April of 1997 was used exclusively for one of the selected image processing methodologies (Vegetation Indices). It was a complete scene, path 198, row 31, covering an area of 185×170 km. Only bands B3 (0.63-0.69 μm, red) and B4 (0.76-0.90 μm, near infrared) were used. To match the other data sets, TM were resampled to a final spatial resolution of 25 meters. A 974 column by 1984 row sample subsection, corresponding to the fire are and its surroundings, was finally extracted from both images, and employed in the processing techniques.

2-Aerial photography: 410 color and infrared aerial photographs were taken from a small airplane with a conventional camera, without the objective of photogrammetric restitution (Masip 2001). The area covered by these photos was approximately of 7500 ha, with an approximate scale of 1:3250, depending on the airplane height. Spatial horizontal overlap reached values of 50 percent (Masip 2001). These photos were taken during several flights in the month of March of 1999, as part of a restoration project for the burned area (Casas et al., 1999). By visual interpretation, an orthophotomap, and the help of a GIS system, these photographs were used to obtain a geo-registered vector of 1-pixel ground control points (GCP), to check for the accuracy of the resulting image classifications.

3- Field survey: As a part of a restoration research project for the El Solsonès fire (Casas et al., 1999), a field survey was developed during Spring of 1999. One of the objectives of this restoration research was to characterize the level of forest damage. Severity classes were delimited using mountain slopes as the spatial sampling unit. The outcome of this survey was given as a digital vector, at a 1:250000 scale (Casas et al., 1999), which was transformed into a 974 column × 1084 rows raster layer, with a spatial resolution of 25 m. Because this field survey focused on fire damage inside the fire perimeter, no data were available outside this boundary.

Additional digital data used in this study included orthophotomaps (1:25000) (ICC 1993), a land cover map from 1992 (25 m-pixel resolution), and a Digital Elevation Model (DEM) (45 m-pixel resolution). All these layers were finally resampled to 25 m pixel. A fire polygon of the burned area was used to mask the final classified images, in order to enhance comparisons with the field survey information, that did not present data outside the fire boundary.

Image pre-processing

Both pre-fire (LANDSAT-TM) and post-fire (IRS-LISS-III) satellite images were geometric and radiometrically corrected by means of MIRAMON 4.0 (Pons, 2000). For the geometric correction, more than 50 control points were selected in the IRS scene, and a polynomial and a digital elevation model technique

was applied (Palà & Pons 1995 model), using a nearest neighbor resampling method. The scene was georeferenced to a NAD83 UTM coordinate system with a root mean square (RMS) error lower than 1 pixel. An image-to-image correction was applied to the TM subscene, with a final RMS error lower than 1 pixel. The radiometric revision implied absolute corrections: digital numbers to radiance values (standard gain and offset coefficients) and radiance to reflectance values (scaled to 0-255), with the radiometric correction model of Pons and Solé-Sugrañes (1994). When multitemporal comparisons were required, even though images were calibrated to a reference atmosphere, a final normalization by means of invariant training areas in both images was applied, and least-square linear regressions were calculated. The objective was to minimize any remaining atmospheric bias, as well as multisensor differences, thus allowing comparisons among images. Parameters for the regression equations are shown in Table 1.

Table 1: Linear equations obtained from invariant targets in the 1997 TM image and 1998 LISS-III image, in order to adjust it from possible atmospheric biases. 1997's image was taken as the reference image (X), while 1998 was the dependent image (Y).

LISS-III (IRS-1C) band	B2_98-97	B3_98-97	B4_98-97	B5_98-97
Linear equations	$y = 0.8721x + 22.594$	$y = 0.9553x + 14.144$	$y = 0.8856x - 0.1269$	$y = 1.1608x + 9.419$
R-square adjustment	$R^2 = 0.9755$	$R^2 = 0.9844$	$R^2 = 0.9774$	$R^2 = 0.9301$

Image processing

1- Simple Spectral Mixing Analysis (SMA)

SMA models a spectrum as a combination of spectra from several pure materials, weighted by the proportion of each material within the IFOV. Pure spectra are known as “endmembers” and can be derived from the image or the field (Adams et al. 1986, Sabol et al., 1992, Roberts et al., 1993). The most common approach is to assume linear unmixing, although non-linear mixing can occur (Adams et al., 1993; Roberts et al., 1993). Endmember selection is an iterative procedure that searches for that combination of pure materials that minimizes fraction overflow (values higher than 1) and underflow (values below 0) and provides the best fit, expressed as a Root Mean Squared Error (RMSE). Overflow indicates the existence of purer materials in the image, while a high RMSE shows pixels that are not well modeled by the endmembers. In our study, final fractions were allowed to be negative or superpositive (greater than 1). The value of the RMSE must be lower than the level of noise in the system, in order to guarantee the viability of the results. LISS-III signal-to-noise value is approximately 2 DN. For its sub-pixel analyses, SMA has the potential of producing results that are directly related to post-fire land management (Caetano et. al 1994; Cochrane and Souza, 1998). Among its limitations, the selection of endmembers, spectral ambiguity between important materials (ie, NPV and Soils, charcoal and shade) and limits on the number of endmembers that can be included in a model are the most important (Sabol et al., 1992; Roberts et al., 1993; Mather 1999). In this study, four endmembers were selected: charcoal, soil, green vegetation and shade (Figure 2). Even though these endmembers represent the major components of interest, fraction overflow was expected, due to the diversity of soil colors and phenological variation of the vegetation. Regarding the selection of an

endmember for the burned area, Caetano et al., (1994, 1996), Retzlaff (2000), as well as this study, consider charred vegetation (graphitic black carbon) as the burned endmember for a Mediterranean fire, while Roberts et al., (1998), Cochrane & Souza (1998) and Rogan et al., (2002), used non photosynthetic vegetation in a Brazilian landscape, for the same purpose. In the case of the non photosynthetic vegetation endmember, confusions with soils have been reported (Roberts et al., 1993); while they have also been reported in the case of the graphitic black carbon, with shade (Retzlaff 2000).

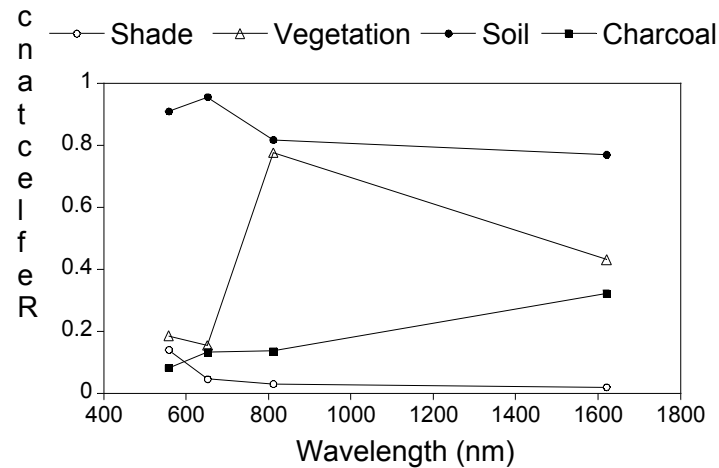


Figure 2: Reflectance values for the pure endmember selected for the SMA procedure: charcoal, photosynthetic vegetation, shade and soil spectra.

2- Vegetation Indices

Two band ratio-based vegetation indices (VI) rely on the differential spectral response of red and near-infrared bands on vegetated and non-vegetated surfaces to detect and characterize burned areas. Thus, the sharp spectral change over burned areas helps to detect burned land (Kasischke et al 1993), while differential spectral responses between red and NIR or SWIR bands, supposedly help determining burned severities (Pereira et al., 1999). The main limitations of this methodology result from non-linear relations between vegetation properties and spectral variations; mathematical limitations on the structure of the indices; and a myriad of sources of noise (Huete 1986; Kaufman & Tanre 1992; Xia 1994; Chen 1996; Purevdorj et al., 1998). In this study, three ratio-based indices are evaluated, the Modified Simple Ratio (MSR, Chen 1996), the Normalized Difference Vegetation Index (NDVI, Rouse et al 1973) and the Second Modified Soil Adjusted Vegetation Index (MSAVI2, Qi et al., 1994b). These three indices were chosen for their different abilities to minimize soil and atmospheric noise, and because they contain different information of vegetation characteristics.

1) The Modified Simple Ratio is a non-linear index, as it uses a non-linear combination of red and NIR reflectance. It was created to correct frequent non-linear relations between vegetation indices and surface physical parameters of vegetation (Chen 1996).

$$MSR = \sqrt{[(NIR/RED) - 1] / [(NIR/RED) + 1]}$$

(1)

2) The Normalized Difference Vegetation Index is a frequently used index that favors the reduction of noise, due to its ratio-structured formula. One of its limitations refers to frequent non-linear relations between NDVI and biophysical parameters (NDVI increases slower than biophysical parameters) (Chen & Cihlar 1996, Chen 1996). For this reason it is expected that MSR will be more linearly related to the parameters than NDVI. Besides, MSR is expected to perform better than NDVI because it is insensitive to the unknown optical and geometrical properties of the vegetated surface (Chen 1996).

$$\text{NDVI} = (\text{NIR} - \text{RED}) / (\text{NIR} + \text{RED}) \quad (2)$$

3) The Second Modified Soil Adjusted Vegetation Index is a non-linear index that was developed by Qi et al., (1994a), as an iterated version of his own Modified Soil Adjusted Vegetation (MSAVI). These modifications of the original SAVI (Huete 1986), attempt to account for differences in soil background, correcting the weakness of SAVI in how vegetation responds, as it moves away from the soil line. MSAVI₂ however, does not require an empirically determined soil line (L) (Chen 1996).

$$\text{MSAVI}_2 = (\text{NIR} + 0.5) - \sqrt{[(\text{NIR} + 0.5)^2 - 2(\text{NIR} - \text{RED})]} \quad (3)$$

These three selected Vegetation Indices (MSR, NDVI and MSAVI₂), were applied to the pre and post-fire images (3x2 layers), subtracting afterwards the pre-fire image to the post-fire image [1998-1997]. These three final subtracted images were masked by the fire perimeter area, in order to make comparisons possible with the Field Survey layer. Only subtracted images were used for quantitative comparisons among methodologies.

3-Texture Filtering

Texture is not easy to quantify since there is neither a consensus on its definition nor a precise mathematical formulation (Soares et al., 1997), moreover, it is a variable strongly dependent on the scale, although it is not necessarily random. The main potentials of this technique refer to its independence upon the type of data, with no requirements about its normal distribution (Mather 1999). It also has a proved ability to improve the overall classification accuracy, compared to spectral classification alone (Dikshit 1996, Ryherd & Woodcock 1996, Soares et al., 1997). In spite of its potential, texture has not always been considered as an aid in image analysis and some authors have suggested its removal from classification procedures (Irons & Petersen 1981). The reason for this are i) the existence of high variance-portions of the image that make classification difficult when treated in a per-pixel fashion (Chusnie 1987 in Ryherd & Woodcock 1996), ii) the difficulty in relating the scale of the spatial resolution of the image, to the scale of the textural feature on the ground, and iii) the edge effect associated with window-based texture technique (Dikshit 1996).

This study will consider co-occurrence measures, calculated as a matrix of relative frequencies of a 5x5 pixel processing window. Eight texture co-occurrence statistics were obtained, using the four bands of the IRS post-fire image: mean, variance, homogeneity, contrast, dissimilarity, entropy, second moment, and correlation. Some of these texture feature have been used as landscape indices to evaluate the complexity

of the mosaic and the contrast between patches (Musick & Grover 1991). More information about these texture features, and their physical meaning, can be found in Haralick et al., (1973) and Soares et al., (1997). 32 final texture layers were obtained (8 for each band), finally applying a mask to focus on the fire area. Initial studies of textures with a 3×3 window were made, but a visual improvement of categories was observed by increasing the window size to 5×5, as it has been described in other studies (Dikshit 1996).

4-Raw Reflectance Data

Raw Reflectance Data has been considered as a useful tool to characterize burned areas, yielding better results than other image techniques (Chuvieco & Congalton 1988; Lawrence & Ripple 1998; Koutsias et al., 1999). Reasons for its ability to outperform other techniques have already been mentioned in previous sections. In our study, Reflectance Data consisted on the original spectral levels of each pixel, after the pre-processing corrections.

Decision Tree classification

As a final step, a tree decision classifier was applied to the classified satellite images, following Roberts et al., 1998, (in press). The purpose was to determine which of the utilized techniques was more useful to characterize the burned land covers, rather than to evaluate the accuracy of this methodology for burned area assessments. The decision tree algorithm is based on a process called recursive partitioning, which consists of dividing the data into two sets that produce the largest decrease in deviance (i.e. measure of heterogeneity) (Andersen et al., 2000). After extracting training data from the user defined classes, it iterates to develop several splitting rules that divide the original data into progressively more homogeneous branches. Binary recursive partitioning continues until the original data has been divided into pure nodes or the remaining data are too sparse. Once the tree has been built, it is commonly necessary to “prune” the tree, in order to reduce complexity by removing redundant branches or those branches with few points and minimal increases in accuracy. After building the tree, the splitting rules can then be entered into a separate program and applied to the original data. Since the objective of using a tree classifier was to assess which image processing technique had a higher weight in the determination of the land cover classes, splitting rules were not finally applied to the classification of the whole image. 26 different layers were included in this tree analysis: Vegetation indices classified images (9 total layers: 3 pre and 3 post-fire layers and their 3 correspondent subtractions), the spectral mixture analysis (5 layers: green, soil, burned, shade and RMS), the textural features of the best performing band (band 2) (8 layers) and the raw reflectance bands (green, red, near infrared and middle infrared).

Steps in the classification procedure

In order to compare the ability of each methodology to characterize the burned area, three *pure* land covers were chosen for the map legend: soils, burned areas and surviving forested areas within the fire perimeter -more than 50% of their crowns alive-. Due to the ecological importance of mixed areas, where burned and unburned vegetation combine, a fourth *non-pure* class was selected, labeled as the mixed class.

It includes all those areas where fire had a patchy behavior, resulting in a heterogeneous combination of fire severities, over a range of soil levels. The degree of heterogeneity, however, depended on scale: slopes in the case of the Field Survey and pixels in the case of the images. This heterogeneity complicated comparisons among methods.

All processing techniques were applied to the post-fire LISS-III image, with the exception of the Vegetation Indices, that were also applied to the pre-fire TM image. Processed images were finally classified into the four classes, by means of a Maximum Likelihood (ML) classifier. The reason for utilizing a classifier algorithm was to avoid a subjective, non-physical selection of each class, by density slicing or thresholding. Eight training targets were selected to represent the variability of the study area: burned areas, soil (2 different targets), green vegetation (3 targets), mixed pixels and water. The selection of water was necessary due to the existence of a reservoir in the image subset. Brightness differences required the selection of two types of soils and three categories of green forests. Once the ML classifier was applied, images were masked by the fire perimeter to favor comparisons with the Field Survey methodology, which did not have data outside the burned area.

To compare the relative performance of the different methodologies, 740 ground control points were chosen from the available aerial photography, in a stratified random design. In those areas where there could be changes related to the time lag between the images and the photos (i.e. unburned green islands), limitations were minimized selecting those areas where minimum changes had occurred (i.e. center pixels of unburned green islands). From the original ground control points, approximately 200 control points were randomly chosen for each class, with the exception of mixed areas, where fewer control points were available. The selection of the 200 points for the pure classes was done by means of a discrete uniform distribution function (SPSS 10.0).

The accuracy assessment was based on confusion matrices and the KHAT statistic (Congalton 1991). This statistic indicates if the confusion matrices of each layer are significantly different from a random result. Kappa analyses -and its KHAT statistic- can also be used to compare different matrices from different classifiers (Smits et al., 1999) and to determine statistical significant differences among classifications, by means of the Z statistic test (Smits et al., 1999). Other accuracy statistics were also considered: The Overall Accuracy (O.A), the Producer's Accuracy (omission error), which indicates how well the training points were classified; and the User's Accuracy (commission error), indicating the probability that a classified pixel actually represents that category in reality. Due to the heterogeneity of the mixed class, low accuracies were expected when the *non-pure* class was included with the *pure* classes. For this reason, two accuracy assessments were separately established, one exclusively dealing with *pure* classes, and another dealing with *pure* and *non-pure* classes, in order to observe the effect of incorporating that mixed class. Most of the processing work was performed using ENVI 3.0 and the GIS system MIRAMON 4.0vh (Pons, 2000).

RESULTS

Class characterization

Confusions among pure classes occurred for all methodologies, even though pure classes were supposedly quite different in their spectral responses. The burned class was most often confused. Thus, *burned land* was confused with soils based on the Vegetation Indices, with MSAVI2 showing the least number of problems (Figure 3). Interestingly, this last index yielded higher values for the soil class than for the burned area. Soils were, therefore, the class with the greatest change in this technique. For the Raw Reflectance Data and the Textural trends, the burned area was mainly confused with the unburned green islands. In the texture technique, these two classes displayed similar values, although separability was possible in band 2 (Figure 4). In the case of the Raw Reflectance Data (Figure 5), the burned land and the unburned green islands were confused in the visible range (reflectance values of 15%), while displayed different behaviors in the near-infrared band (BD4). In regard of the *green islands class*, the Spectral Mixing Analysis displayed lower values than expected, in its fraction of photosynthetic vegetation for this unburned islands class (0.25) (Figure 6). For the texture analysis, this green class and the soil class displayed the most contrasted behaviors: the lowest contrast and dissimilarity values, and the highest homogeneity, second moment and correlation (in absolute values) for the unburned green islands, and the opposite trend for the soils. The angular second moment for the green band (BD2) was the best performing texture measures to separate unburned islands, as indicated by the tree classifier. Regarding the *mixed class*, the SMA technique displayed mixed areas characterized by a large amount of soil and charcoal with some photosynthetic vegetation. In the Raw Reflectance Data, mixed areas presented higher reflectances than the unburned and burned classes, due to the presence of soil. In the case of the Textural analysis, contrast, homogeneity, correlation and dissimilarity values indicated more homogeneity than soils for this mixed class, and less than unburned or burned areas.

Class areas

Figure 7 (A-E) displays the five classified images obtained in this study: Field Survey, Spectral Mixing Analysis, Raw Reflectance Data, Vegetation Indices, and Texture Filtering. Total areas of each methodology depend on the combined ability of the ML classifier and the potential of each technique to separate among classes. Total areas of each class and their percentages are shown in Table 2. The main difference among the areas of the pure classes refers to the amount of unburned and burned areas. SMA and Reflectance Data displayed the highest values for the unburned class, being 2.5 and 2 times larger than the Field Survey, which presented the lowest value (Table 2). For the burned class, Texture was the technique with the lowest area, while maximum values were reported for the Vegetation Indices (Table 2). Considering the soil class, SMA was the classification method with a larger deficit, while Texture presented the highest value. As expected, the non-pure category was the less homogeneous, in terms of total area, being maximum for the Texture methodology and minimum for the Vegetation Indices.

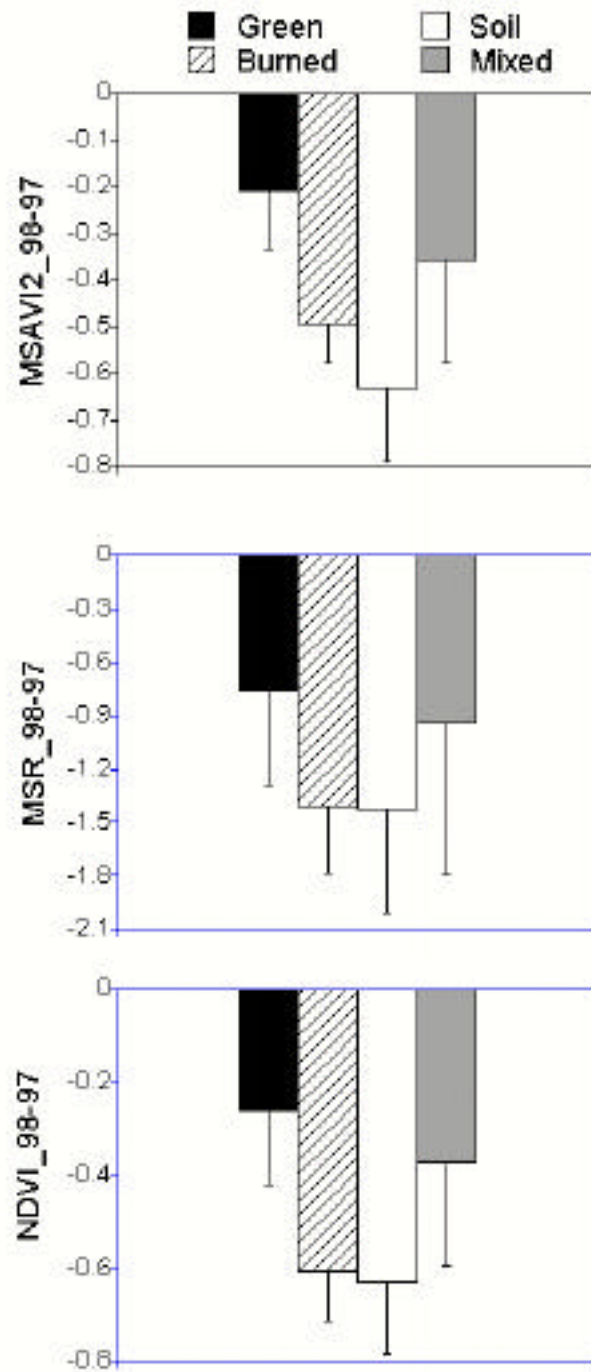


Figure 3: Mean values and standard deviations of each class, for the Vegetation Indices technique. The vertical arrangement represents MSAVI2, MSR and NDVI respectively. Bars correspond to each class: green, burned, soil and mixed land.

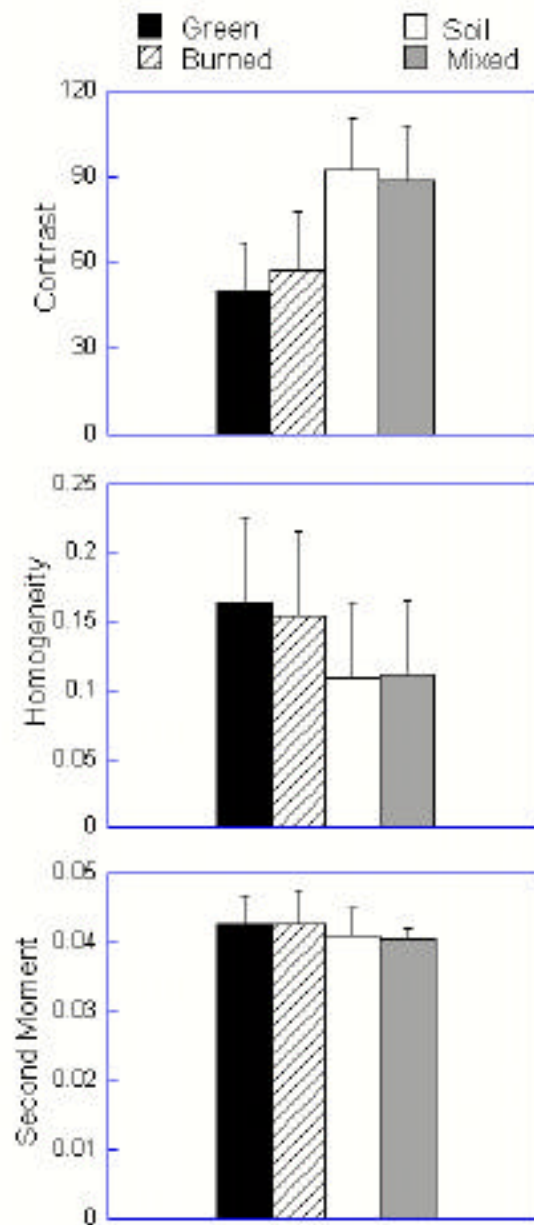


Figure 4: Mean values and standard deviations for three selected texture statistics, for band 2. The selection of this band related to a better separability among classes, compared to the rest of bands. In vertical order, the statistics that appear are Contrast, Homogeneity, and Second Moment.

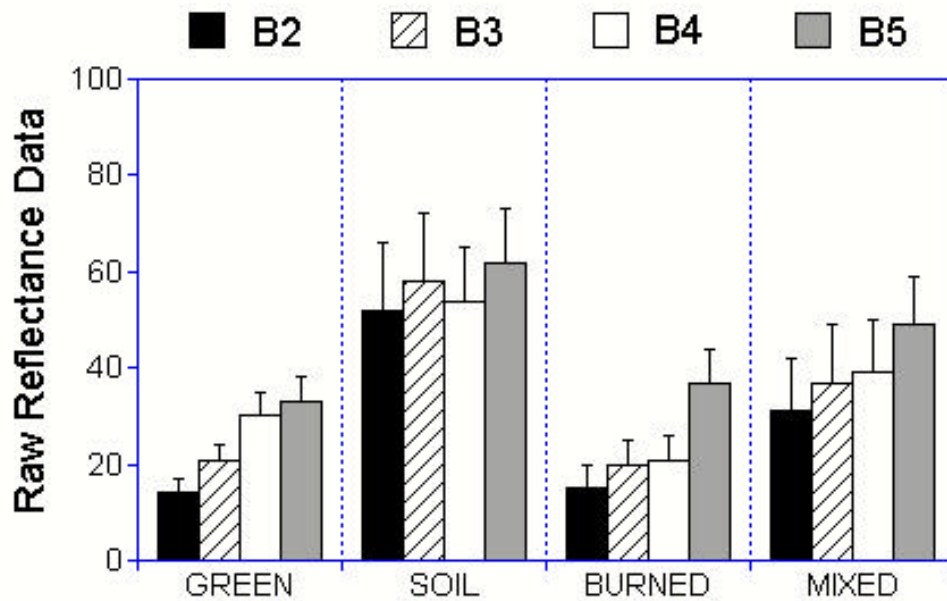


Figure 5: Mean values and standard Deviations for each class, for the Reflectance Data technique. Bars represent the utilized different bands: B2, B3, B4 and B5.

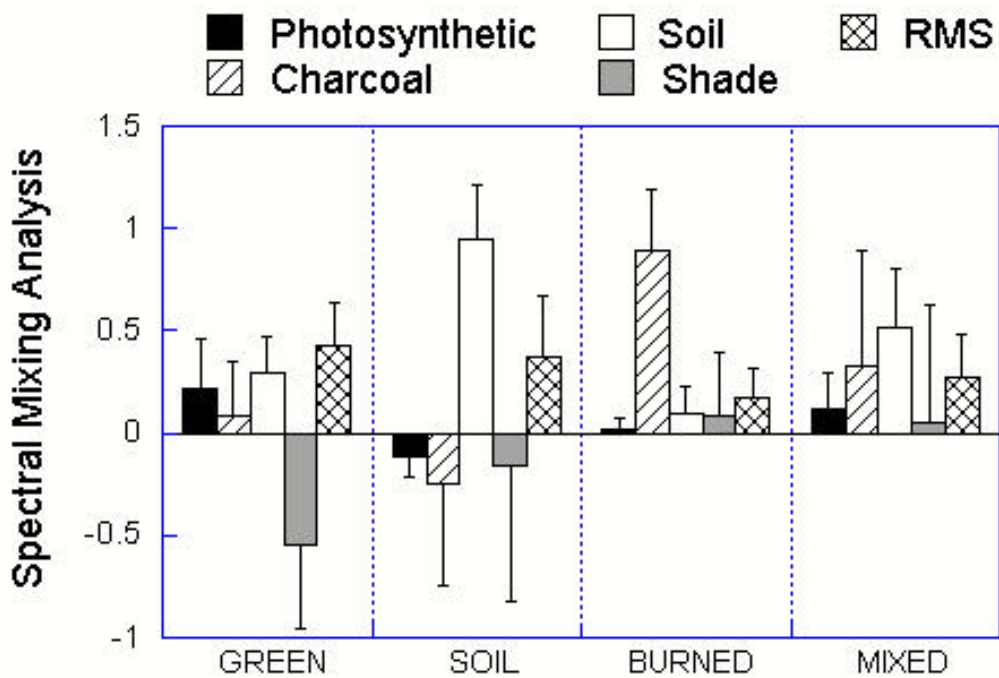


Figure 6: Mean values and standard deviations for each class, for the SMA technique. Bars represent the different endmembers: photosynthetic, charcoal, soil, shade, and the error term (RMS). Each sub-section in the graphic divides the four selected classes: green, soil, burned and mixed land.

Table 2: Areas for each pure and non-pure class, in hectares and percentages, for every selected methodology. The category “Others” refer to browned toasted pines, whose needles have dried out, remaining on the tree, in the Field Survey; while they refer to water confusions and unclassified pixels in the remaining methodologies.

Methods	Unburned		Soil		Burned		Mixed		Other		Total ha
	ha	%	ha	%	ha	%	ha	%	ha	%	
Field Survey (FS)	1148	4.5	7332	28.9	11967	47.2	4414	17.4	1465	2.0	26327
Spectral Mixing Analysis (SMA)	2868	10.9	5710	21.7	11012	41.8	6627	25.2	110	0.4	26327
Vegetation Indices (VI)	1657	6.3	7022	26.7	14665	55.7	2416	9.2	567	2.2	26327
Reflectance Data (RD)	2259	8.6	6073	23.1	11455	43.5	6505	24.7	35	0.1	26327
Texture Filtering (TF)	1302	4.9	7363	28.0	7731	29.4	9835	37.4	96	0.4	26327

Accuracy assessments

When exclusively focusing on the *pure* classes (unburned areas, soils and burned areas), all methods displayed high *Overall Accuracies*: The field survey offered the lowest value (68.6%) whereas SMA and the Reflectance Data (RD) presented the highest (82%) (Table 3). When both pure and non-pure classes were considered, *Overall Accuracies* decreased around 30-40%, depending on the method (Table 3). Texture accuracies showed the greatest decrease between the three class and four class maps, while the rest of techniques showed similar low accuracies (Table 3).

Regarding the *KHAT statistics*, the highest values corroborated the Overall Accuracy results, with SMA and Reflectance Data showing the highest accuracies ($k=0.721$ and $k=0.718$ respectively), followed by the Field Survey method ($k=0.602$). Texture and Vegetation Indices displayed considerably lower kappa values ($k=0.56$ and $k=0.53$, respectively). A revision of significant differences among KHAT statistics –based on the Z statistic- (Table 4), revealed that Texture, Vegetation Indices and the Field Survey classifications were not significantly different in accuracy, whereas SMA and Reflectance Data were significantly better (Table 4). When the mixed, non-pure class was introduced, KHAT values displayed unacceptably low values. With this fourth class included, all techniques were better than Texture, and not significantly different from the Field Survey (Tables 3 and 4). A revision of significant differences among all considered methodologies, revealed that all classifications exclusively dealing with pure classes, were significantly better than the four-class classifications, for all methodologies (Table 4).

Individual Class Accuracies revealed diverse differences among methodologies, when pure classes were considered (Table 5). Based on the User’s Accuracy, SMA and Reflectance Data were the only methodologies with individual accuracies above 75%, for all pure classes (Table 5). In the case of unburned areas, individual accuracies were high, above 75% for all methods, with Texture and Vegetation Indices, the most accurate. These last two techniques, together with the Field Survey also displayed the highest omission errors (Table 5). In general terms, this unburned class was characterized by the highest omission errors of all pure classes, and was responsible for the differences in total unburned areas, ranging from 1148 to 2868 ha (Table 2). The burned class was the one with highest commission errors (lowest User’s Accuracy, Table 5), mainly associated with the Vegetation Indices and the Field Survey. Revising the confusion matrices, green

and soil classes were the main sources of confusion. Soil classifications were accurate in almost all methodologies (82%). The exception was the Texture method, with a lower soil accuracy (68%), although its omission errors were the lowest (Table 5). Burned areas were the most frequent source of confusion of this soil class. When the mixed class was incorporated into the confusion matrix, its individual accuracy was unacceptably low (Table 5).

Table 3: Overall accuracies, KHAT statistics and their upper and lower confidence limits, for each considered methodology, for both the pure classes: unburned class, soil and burned areas and the pure and non-pure classes: unburned class, soil, burned and mixed areas.

Pure classes	Overall Accuracy	KHAT	Lower Limit	Upper Limit
Field survey (FS)	68.64	0.602	0.540	0.665
Spectral Mixing Analysis (SMA)	82.03	0.721	0.665	0.778
Vegetation Indices (VI)	70.12	0.534	0.472	0.596
Raw Reflectance Data (RD)	82.06	0.718	0.660	0.775
Texture co-occurrence (TF)	72.41	0.563	0.489	0.637
Pure and non-pure classes	Overall Accuracy	KHAT	Lower Limit	Upper Limit
Field survey (FS)	53.81	0.388	0.337	0.438
Spectral Mixing Analysis (SMA)	56.78	0.421	0.372	0.471
Vegetation Indices (VI)	56.98	0.392	0.340	0.446
Raw Reflectance Data (RD)	56.69	0.418	0.368	0.467
Texture co-occurrence (TF)	42.83	0.255	0.202	0.307

Table 4: Significant Zeta statistics ($Z = 1.96$) for all possible pair combinations of the considered methodologies. The number 3 refers to each methodology when only pure classes are considered (unburned class, soil and burned areas), while 4 refers to each methodology when both pure and non-pure classes are considered (mixed areas, as the non pure class). * Indicate significant differences between the contrasted methodologies. n.s refers to non significant differences. FS=Field Survey, SMA=Spectral Mixing Analysis, VI=Vegetation Indices, RD=Reflectance Data, TF=Texture Filtering (co-occurrence measures).

	Pure classes				Pure and non-pure classes				
	SMA3	VI3	RD3	TF3	FS4	SMA4	VI4	RD4	TF4
FS3	*	n.s	*	n.s	*	*	*	*	*
SMA3		*	n.s	*	*	*	*	*	*
VI3			*	n.s	*	*	*	*	*
RD3				*	*	*	*	*	*
TF3					*	*	*	*	*
FS4						n.s	n.s	n.s	*
SMA4							n.s	n.s	*
VI4								n.s	*
RD4									*

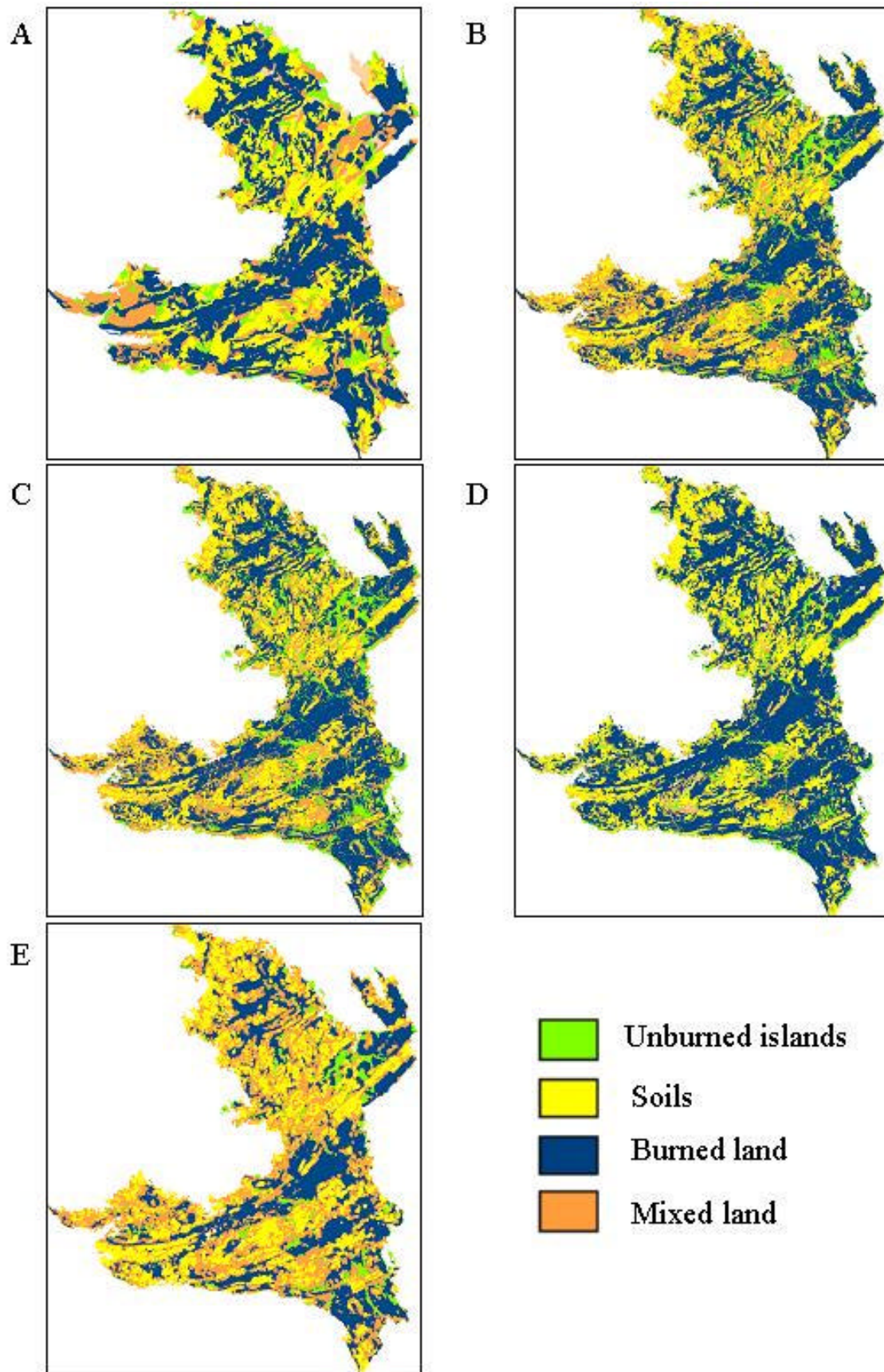


Figure 7: Final classified images obtained by means of the Maximum Likelihood, for all the employed techniques: A) Field Survey, B) Spectral Mixing Analysis, C) Raw Reflectance Data, D) Vegetation Indices, E) Texture, at a scale 1:125000 (approx.). Colors corresponding to each class are indicated in the legend.

Table 5: User's and Producer's Accuracies for each methodology, when only pure classes are considered and when pure and non-pure classes are considered. This separate analysis of pure classes and their combined effect with the mixed class, allows a comparative analysis of both situations, strengthening the importance of dealing with pure classes alone.¹Producer's Accuracy=Omission errors, ²User's Accuracy=Commission Errors.

	Pure classes			Pure and non-pure classes					
		Unburned	Burned	Soil	Unburned	Burned	Soil	Mixed	
Field survey (FS)	¹ P	54.17	87.27	73.71	¹ P	32.50	70.94	70.1	12.1
	² U	76.47	64.57	87.73	² U	67.53	54.96	86.1	5.9
Spectral Mixing Analysis (SMA)	P	70.90	87.93	82.88	P	42.69	75.00	60.8	21.7
	U	82.95	77.27	88.32	U	76.84	65.11	86.4	7.92
Vegetation Indices (VI)	P	41.73	89.34	71.08	P	34.32	86.00	62.0	5.00
	U	84.06	60.69	82.52	U	81.69	51.76	79.7	4.69
Raw Reflectance Data (RD)	P	68.13	89.71	81.58	P	39.00	77.00	61.0	22.0
	U	81.58	77.34	89.21	U	75.61	65.15	87.3	8.00
Texture co-occurrence (TF)	P	48.05	73.53	85.19	P	23.00	49.00	56.0	28.0
	U	88.10	73.00	68.05	U	82.22	59.17	65.0	7.17

Best performing techniques in the frame of a tree classifier

Figure 8 displays the pruned tree diagram, where the splitting rules to obtain each class can be visualized. Its classification accuracy was of the 88 percent. The statistics required by this classifier to create this tree diagram, were obtained with the same training targets used for the ML classifier. For this reason, there are 8 final classes, which were finally re-organized into the three pure classes and the mixed class. A revision of this tree diagram reveals that the main partitioning of the data relies on brightness differences in the SWIR band (0.38). Dark targets correspond to the left branches of the tree (Figure 8). Water is easily distinguished, while the conifers and the burned land targets are separated by means of the near infrared reflectance (0.22). Confusions between burned areas and conifers can already be noticed at this point. The right branches of the tree diagram corresponded to brighter targets. These targets displayed lower spectral separability, rising the complexity of this part of the tree (high number of terminal nodes) and leading to higher levels of noise. The subtraction of NDVIs (0.38) and the soil endmember (0.33) basically separate areas with or without soil (right from left nodes) (Figure 8). Areas with large amounts of soils are characterized by the soil endmember (0.33). The texture feature of the Second Moment (0.068) helps differing between mixed land and bright vegetation, while the red band () separates between darker soils and conifers.

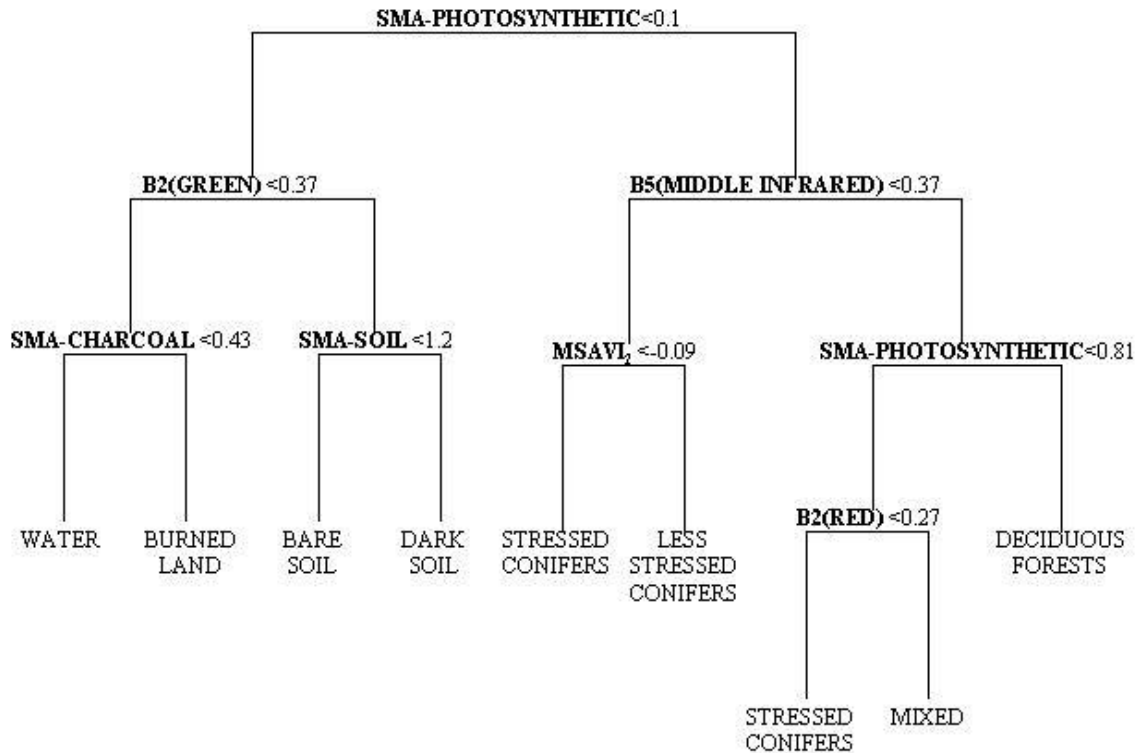


Figure 8: Tree diagram displaying the partial contribution of each technique to the classification of the burned area. There were eight final classes corresponding to the training targets selected for the ML classifier: water, charred areas, conifers, stressed conifers, bright vegetation, bright soil, dark soil, and mixed land. In all processing methodologies, these classes were finally re-organized into three pure classes: unburned islands, soil and burned land, and one non-pure class: mixed areas.

DISCUSSION

When pure classes were considered, the most accurate methodologies were those directly related to the spectral characteristics of the pixel: Reflectance Data and SMA, versus the poorer performances of Vegetation Indices, Textural measures and the Field Survey. Since no image processing technique was applied to the Raw Reflectance Data, it can be considered the most cost-effective methodology, whose importance is reinforced by the tree classifier. The ability of some reflectance bands (mainly red, near infrared and shortwave near infrared) to outperform the classification of other processing techniques, mainly vegetation indices, has long been reported (Chuvieco & Congalton 1988; Chavez & MacKinnon 1994; Mas 1999). In this regard, Lawrence & Ripple (1998), suggest that this ability might be related to an unnecessary constraint of the vegetation indices values, when compared to a wider range of variability offered by 256 grey tonal levels. At the other extreme there are the expensive cost-effective methods, such as the Field Survey and the Texture technique. In the case of the Field Survey, its performance was remarkably lower than that reported in other studies, where both aerial photography and field survey displayed better accuracies than VI (Rodríguez-Silva et al., 1997). Martin et al., (1999) point out that traditional ground-based visual detection methods are not always appropriate for the identification of fire location, size and intensity, due to the small field of view that can be obtained from the ground. Moreover, typical problems diminishing

the accuracy of field work refer to the assignation of visual damage in the field and the location of some parcels in places with no homogeneous illumination nor vegetation conditions, enhancing the problem of class characterization, combined with misregistration errors (Rodríguez-Silva et al., 1997). Derived features, such as texture, might be expected to display a higher degree of spatial autocorrelation than the individual pixel values in the raw image, because of the use of overlapping windows, diminishing its accuracy (Mather 1999).

Part of these accuracy differences among methodologies refer to the ability of each technique to cope with several sources of errors that are introduced in diverse stages of the pre-classification, classification and post-classification (Lunetta et al., 1991, Smits et al., 1999). In our study, the major *pre-classification* errors relate to the experimental design. In particular, the spatial scale of the Field Survey, with “slope” as the sampling unit. This unit was much less exhaustive than the pixel-based methods, which considered minimum areas that were 20 times smaller (0.06 ha) than the minimum size of the patches of the Field Survey. This scale problem was the reason that small unburned patches were not considered in the Field Survey, corroborated by the omission errors of this class, which were the highest of all methods (Table 5). Furthermore, considering that the aerial photography was obtained at the same time as the Field Survey, this lower spatial resolution had a larger influence on the quality of the data than the temporal lag between the satellite images and the Field Survey. Another major problem in our study was the difficulty in characterizing a common non-pure class, both for the field survey and the satellite images. Thus, this mixed class had to account for the problem of the mixed pixel, which, at different scales, corresponded to different interpretations: in the case of the Field Survey, this non-pure class represented those areas with a heterogeneous fire behavior, where patches of diverse severities were left; for the satellite imagery, this non-pure class responded to pixels (625 m²) that included diverse affectations, as a consequence of different fire types. This forced the loose definition of this class and suggested the need to focus on the pure classes for accuracy assessments.

When considering possible sources of error associated to the *classification* procedure, three major ones were detected: i) the use of the maximum likelihood classifier, ii) the presence of a strong dark background, and iii) technical constraints of some methodologies. The maximum likelihood classifier was selected because it is a commonly used and is a robust classification technique (Milne 1986). However, this algorithm assumes a normal probability distribution of the data (Mather 1999), which is unlikely to be accomplished by all image techniques, especially Texture and Vegetation Indices. Therefore, caution is required when interpreting the results. Another source of confusion refers to the loss of contrast between the burned target and the background, in the visible range, resulting in a poor differentiation of dark land covers (Tanaka et al. 1983, Chuvieco & Congalton 1988, Pereira et al., 1999). The presence of a strong dark background, reduced the reflectance of those unburned patches included inside the fire, as had previously been reported by Razafimpanilo et al., (1995) and Ni et al., 1998 (in Pereira et al., 1999). These authors pointed out the difficulty in distinguishing unburned vegetated patches inside a burned matrix, independent of the green stand density. In this regard, Kaufman (1989) reported the importance of the adjacency effect, in which the radiance measured from a target is modified by scattered radiation from an adjacent area, which can lead to

an increase or decrease in radiance depending on the brightness of the surrounding background, the size and distribution of those surrounding elements, the aerosol optical thickness, and the technical properties of the sensor (i.e. field of view, observation angle, etc). This last author demonstrated how the atmospheric effect in the presence of non-uniform and/or non-Lambertian surfaces (i.e. vegetation), can reduce the separability among spectrally different classes, affecting the classification procedure. In our study area, charred areas were frequently surrounded by bright soils, enhancing this phenomena.

The darkening effect observed in our study, was partly the reason for the low fraction of the green endmember, in the unburned class. The other part related to the much darker response of the main surviving species -conifers-, when compared to the bright green endmember selected, and the impossibility of correcting its shade content (see below). Reflectance Data was also affected, displaying a better characterization of each class by means of the NIR and SWIR bands, than by the visible range (Figure 5). This darkening effect can be related to the higher impact of uncorrected atmospheric scattering in the visible range, over dark land covers, producing atmosphere-induced variations on canopy spectra, which can exceed those due to vegetation characteristics (Huete 1986; Qi et al., 1993). This effect produces a reduction in several Vegetation Indices values (i.e. NDVI) which is greater for increasing atmosphere turbidities and decreasing canopy background brightness (Huete & Jackson 1988). In our study, this effect was enhanced by the lack of rain and very stable conditions after fire, determining the presence of aerosols from the burning process, one month after the fire. The use of atmospheric resistant Vegetation Indices might have minimized these atmospheric biases (Miura et al. 2001), although the soil background and the selection of a proper aerosol model would have conditioned their ability.

The third source of classification errors in our study relates to technical limitations of several methodologies, including edge effects associated to the window-based Texture techniques (Dikshit 1996); enhanced spectral noise in the Vegetation Indices; and the confusion between endmembers in the case of the SMA. In this latter case, even though Caetano et al., (1994) successfully used the shade endmember to normalize the fractions of the remaining endmembers, in the present study and in Retzlaff (2000), the shade spectral response was confused with the charcoal endmember, and thus could not be removed through normalization. As a consequence, the physical relationship between fractions and percentages of each endmember were affected, and unreasonable shade fractions were obtained for the brighter classes (i.e soils and unburned class), which presented shade underflows (negative fractions). For these reasons, a classification technique that took into account the physical meaning of the endmember fractions would not have been appropriate, while the use of the Maximum likelihood algorithm avoided these problems. For the Vegetation Indices, atmospheric and soil brightness effects account for the major sources of external noise in our study area (Huete 1986; Kaufman & Tanré 1992). Reported confusion between soils and burned areas refer to spectral changes between the pre and post-fire images, with similar ranges of variation. Productive fields in the pre-fire image were already tilled in the post-fire image, leading to large spectral changes due to the removal of the vegetation. The ability of the MSAVI₂ to better separate these two classes probably relies on the major importance given to the Near Infrared (NIR) band in its equation, while the red band contribution is fairly reduced. Thus, spectral responses in the NIR and MIR band have been reported to better contribute to burn mapping than visible ranges (Pereira et al., 1999).

Regarding the edge effect of the Texture technique, it has been described that all window-based texture measures calculate the average property within the window (Dikshit 1996). Thus, when it comprises more than one class, the computed textural value will not be representative of any of them. This phenomenon occurred wherever there was a class edge in our study, and was responsible for reducing the real area of our most abundant class, the burned area -the one with larger boundaries-, while increasing the mixed one (Table 2). This edge effect partly explains why the mixed class in the textural classification displays the highest area of all methodologies (Table 2, Figure 4). Moreover, this edge effect creates a textural gradient that will reach a plateau at a given distance from the boundary, determining that each pure class, is formed by the core pixels of each patch. For this reason, this texture technique could be considered a “conservative” classification for the unburned and soil classes, only including the central pixels and avoiding the boundaries, where the confusion is detected. This was corroborated by the unburned class, which displayed the lowest commission error and the second highest omission error of all techniques (Table 5).

Among the post-classification sources of error, the most critical is related to the use of point data for accuracy assessment. Even though some authors prefer the use of point data instead of polygons as ground targets (Wilson 1992, Gong et al 1996), points can bias the accuracy results in our study. This relates to the heterogeneity of our landscape, together with potential misregistration errors. However, due to the reduced size of many patches inside the burned area, it was preferred to work with points. Another aspect refers to the loose definition of the mixed class, complicating a proper characterization of these areas and its consequent selection as control points. Finally, the importance of adjacency effects can influence the supervised classification when the training targets have been selected on the ground. Thus, the classification may not be accurate even if the separability between classes is good, due to a difference between the atmospheric characteristics in the classified and the supervised data set (Kaufman 1989).

As a final overview of the selected methods of this study, the low accuracy value of the Field Survey, reveals that time consuming and expensive methods are not necessarily the most accurate, especially when potentially easily distinguishable classes are involved. This is especially true when considering that high resolution images display a synthetic view of these complex field situations, making possible a quicker and cheaper evaluation of the affected area than the one provided by traditional methods of fire effects assessment (Koutsias et al., 1999). This advantage can be highly appreciated in a forest management context, where simple maps, quickly supplied are required for decision making (Koutsias et al., 1999). In the case of burned land assessment, however, certain caution is required, due to the adjacency effect of the strong dark background, which is likely to reduce the radiance of the targets under study (Kaufman 1989). This effect will require the application of atmospheric corrections that do not assume a uniform surface (see review in Kaufman 1989), which frequently need information about the atmosphere that is not available. An adequate selection of the date of the image, will help minimizing some of these errors. Among the large amount of image processing techniques that are applied to characterize burned areas, some of the simplest techniques can be the most cost-effective, as was demonstrated by the supervised classification of the Raw Reflectance Data, in our study. Besides, the use of alternative ways to determine the weight of each technique, in the classification procedure, will help selecting those techniques that are more efficient in the

characterization of burned areas. In our study, the Raw Reflectance Data appears as the most useful technique for classifying burned areas, contributing with half of the total variables that were selected by the tree classifier. The importance of the Middle Infrared Band was demonstrated in the diagram corroborating other studies.

Considering future climatic scenarios (IPCC 2001), as well as the socioeconomic characteristics of many of these frequently burned areas, forest fires will continue being a major disturbing agent in many ecosystems, leading to changes in their structure and functionality, as well as on global climate. For this reason, the analysis of sources of error that difficult the assessment of burned areas, and the quantitative comparison of potential techniques for that purpose, are important and urgent tasks.

ACKNOWLEDGEMENT

This research was partly supported by a Governmental grant (BEAI grants-2000. BEAI200111). Our gratitude to personnel in the Geography Department in University of California, Santa Barbara for their support. To Jose Luis Ordóñez for helping with the figures, to Rafael Rodríguez, Francesc Llimona and field workers, for kindly sharing their Field Survey map of the burned area. To Emilio Chuvieco for the program of matrix normalization and variance elaboration. Our sincere gratitude too to Izayas Numata for his help with the final tree.

REFERENCES

- Adams, J. B. Smith, M. O. and P. E. Johnson (1986). "Spectral Mixture Modeling: A New Analysis of Rock and Soil Types at the Viking Lander 1 Site." *Journal of Geophysical Research* 91(B8): 8098-8112.
- Adams, JB, Smith, MO and Gillespie, AR (1993), Imaging spectroscopy: Interpretation based on spectral mixture analysis, In Pieters C.M., and Englert, P., eds. *Remote Geochemical Analysis: Elemental and Mineralogical Composition 7*: 145-166, Cambridge Univ. Press., NY.
- Adams, J. B., Sabol, D. E., Kapos, V., Almeida, R. Filho, Roberts, D. A., Smith, M. O. & Gillespie, A. R. (1995). Classification of multispectral images based on fractions of endmembers: Applications to land - use change in the Brazilian Amazon. *Remote Sensing of Environment*, 52, 137-154.
- Andersen, M.C., Watts, J.M., Freilich, J.E., Yool, S.R., Wakefield, G.I., McCauley, J.F. and Fahnestock, P.B. (2000). Regression-tree modeling of desert tortoise habitat in the central Mojave Desert. *Ecological Applications*. 10: 890-900.
- Cahoon, D.R. Jr., Stocks, B.J., Levine, J.S., Cofer, W.R. & Chung,C. (1992). Evaluation of a technique for satellite-derived area estimation of forest fires. *Journal of Geophysical Research*, 97, 3805-3814.
- Caetano, M.S. (1995). Burned vegetation mapping in mountainous areas with satellite remote sensing. MA Thesis, University of California, Santa Barbara (UCSB), California.
- Caetano, M.S, Mertes, L., & Pereira, J.M. (1994). Using spectral mixture analysis for fire severity mapping. *Proceedings of the 2nd International Conference on Fire Research*, Coimbra, Portugal, pp.667-677.

- Caetano, M.S., Mertes, L.A.K., Cadete, L. & Pereira J.M.S. (1996). Assessment of AVHRR data for characterizing burned areas and postfire vegetation recovery. EARSEL International Workshop: Remote Sensing and GIS Applications to Forest Fire Management. Alcalá de Henares, Spain.
- Casas, M., Domingo, F., Rodrigo, E., Mora, Francesc, Olarieta, R., Roca, J., Rodríguez, R., Usón, A. (1999). Pla de restauració de la coberta vegetal de la zona afectada per l'incendi del Solsonès: cartografia i avaluació del risc d'erosió i degradació de sòls. Publ. Universidad de Lleida, Lleida.
- Chavez, P. & MacKinnon, D. (1994). Automatic detection of vegetation changes in the Southwestern United States using remotely sensed images. *Photogrammetric Engineering and Remote Sensing*, 60, 571-583.
- Chen, J.M. (1996). Evaluation of Vegetation Indices and a Modified Simple Ratio for Boreal Applications. *Canadian Journal of Remote Sensing*, 22, 229-239.
- Chen, J.M. & Cihlar, J. (1996). Retrieving leaf area index on boreal conifer forests using Landsat TM images. *Remote Sensing of Environment* 55, 153-162.
- Chuvieco, E., & Congalton, R. (1988). Mapping and inventory of forest fires from digital processing of TM data. *Geocarto International*, 4, 41-53.
- Chuvieco, E. (1996). *Fundamentos de teledetección espacial*. 3a Ed. Ed Rialp. Pp: 565.
- Crutzen, P., & Goldammer, J. (1993). *Fire in the Environment, the ecological, atmospheric & climatic importance of vegetation fires*. John Wiley & Sons, New York.
- Cochrane, M.A. & Souza, C.M. (1998). Linear mixture model classification of burned forests in the eastern Amazon. *International Journal of Remote Sensing*, 19, 3433-3440.
- Congalton, R. (1991). A Review of Assessing the Accuracy of Classifications of Remotely Sensed Data. *Remote Sensing of Environment*, 37, 35-46.
- Dikshit, O. (1996). Textural classification for ecological research using ATM images. *International Journal of Remote Sensing*, 17, 887-915.
- Giglio, L., & Kendall, D.J. (2001). Applications of the Dozier retrieval to wildfire characterization: A sensitivity analysis. *Remote Sensing of Environment*, 77, 34-49.
- Gong, P., Pu, R. and Chen, J. (1996). Mapping ecological land systems and classification uncertainties from digital elevation and forest cover data, using neuronal networks. *Photogrammetric Engineering and Remote Sensing*, 62, 1249-1260.
- González, M., & Castellnou, M. (1998). Fuego en la Cataluña Central. *Montes*, 53, 17-20.
- Haralick, R.M., Shanmugam, K. & Dinstein, I. (1973) Textural Features for Image Classification. *IEEE Transactions on Systems Man & Cybernetics*, 3:610-621.
- Hardin, P. & Shumway, M. (1997). Statistical significance & normalized confusion matrices. *Photogrammetric Engineering & Remote Sensing* 63 (6):735-740.
- Harvey, K & Hill, G. (2001). Vegetation mapping of tropical freshwater swamps in the Northern Territory, Australia: a comparison of aerial photography, Landsat TM & SPOT satellite imagery. *International Journal of Remote Sensing*, 22: 2911-2927.
- Hudak, A & Wessman, C. (2001). Textural analysis of high resolution imagery to quantify bush encroachment in Madikwe Game Reserve, South Africa, 1955-1996. *International Journal of Remote Sensing*, 22: 2731-2741.

- Huete, A.R. (1986). A soil adjusted vegetation index (SAVI). *Remote Sensing of Environment*, 25, 295-309.
- Huete, A., & Jackson, R. 1988. Soil and atmosphere influences on the spectra of partial canopies. *Remote Sensing of Environment* 25:295-309.
- Hurcom, S.J & Harrison, A.R. (1998). The NDVI spectral decomposition for semi-arid vegetation abundance estimation. *Int. Jour. Remote Sensing*, 19, 3109-3125.
- ICC. (1993). Institut Cartogràfic de Catalunya. Ortofotomapes 1:25000.
- IEFC. (2000). Inventari Ecològic i Forestal de Catalunya. Regió Forestal IV. CREA, Barcelona.
- Irons, J.R. & Petersen, G.W. (1981). Texture transforms of remotely sensed data. *Remote Sensing of Environment*, 11. 359-370.
- Justice, C.O, Malingreau, J.P., Setzer, A.W. (1993). Satellite remote sensing of fires: potentials and limitations. In Crutzen, P.J., & J.G. Goldammer (Eds). *Fire in the Environment: The ecological, atmospheric & climatic importance of vegetation fires*. John Wiley & Sons, New York. pp:77-88.
- Kasischke, E.S., French, H.F., Harrell, P., Christensen, I. Jr., Ustin, S.L. & Barry, D. (1993). Monitoring wildfires in boreal forests using large area AVHRR NDVI composite image data. *Remote Sensing of Environment*, 45, 61-71.
- Kaufman, Y.J. (1989). The atmospheric effect on remote sensing and its correction. In *Theory and Applications of Optical Remote Sensing* (G.Asrar, Ed), Wiley, New York, pp:336-428.
- Kaufman, Y. & Tanré, J.D. (1992). Atmospherically Resistant Vegetation Index (ARVI) for EOS-MODIS. In *Proceedings of the IEEE International Geoscience and Remote Sensing Symposium '92* (pages 261-270) IEEE, New York.
- Kaufman, Y.J., Setzer, A., Ward, D., Tanre,D., Holben, BN., Menzel,P.,and Rasmussen,R. (1992). Biomass burning airborne and space-borne experiments in the Amazons (BASE-A).*Journal of Geophysical Research* 97:14581-14599.
- Koutsias, N., Karteris, M., Fernández-Palacios, A., Navarro,C., Jurado,J., Navarro, R. & Lobo, A. (1999). Burned land mapping at local scale. In E. Chuvieco (Ed) *Remote Sensing of Large Fires* (pages 157-187), Springer-Verlag, Berlin.
- Lawrence, R & Ripple, W. (1998). Comparisons among Vegetation Indices and Bandwise Regression in a Highly Disturbed Heterogeneous Landscape: Mount St. Helen, Washington. *Remote Sensing of Environment*, 64, 91-102.
- Levine, J.S., Cofer, W.R., Cahoon, D.R., Winstead, E. (1995). Biomass burning: a driver for global change. *Environmental Science & Technology*, 29, 3-12.
- Martín, M.P., Ceccato, P., Flasse, S., & Downey, I. (1999). Fire detection and fire growth monitoring using satellite data. In Chuvieco (Ed) *Remote Sensing of large fires* (pages 101-123). Springer-Verlag. Berlin.
- Mas, J.F. (1999). Monitoring land-cover changes: a comparison of change detection techniques. *International Journal of Remote Sensing*, 20, 139-153.
- Masip, G. (2001). Anàlisi de diferents mètodes de classificació d'una imatge de satèl·lit per caracteritzar la superfície afectada per l'incendi del Solsonès de 1998. Forestry Engineering final project. Universitat de Lleida, Lleida.
- Mather, P.M. (1999). Incorporation of non-spectral features. In *Computer Processing of Remotely-Sensed Images*. John Wiley and Sons, West Sussex, England. pp:198-201.

- Milne, A.K. (1986). The use of remote sensing in mapping and monitoring vegetational change associated with bushfire events in eastern Australia. *Geocarto International* 1:25-32.
- Miura, T., Huete, A., Yoshioka, H., and Holben, B. 2001. An error and sensitivity analysis of atmospheric resistant vegetation indices derived from dark target-based atmospheric correction. *Remote Sensing of Environment* 78:284-298.
- Musick, H.B & Grover, H.D. (1991). Image textural measures as indices of landscape pattern. In *Quantitative methods in landscape ecology* (Eds. Turner, M.G. and Gardner, R.H). Springer-Verlag, New York. Pages:77-103.
- Palà, V. & Pons, X. (1995). Incorporation of relief into geometric correction based on polynomials. *Photogrammetric Engineering and Remote Sensing*, 7, 935-944.
- Pereira, J.M., Sá, A.C., Sousa, A.M., Silva, J.M., Santos, T.N., & Carreiras, J.M. (1999). Spectral characterization and discrimination of burnt areas. In Emilio Chuvieco (Ed) *Remote Sensing of Large Forest Fires* (pages 123-138), Springer-Verlag, Berlin.
- Pons, X. (2000). MiraMon. Sistema d'Informació Geogràfica i software de Teledetecció. Centre de Recerca Ecològica i Aplicacions Forestals, Bellaterra, Spain.
- Pons X. & Solé-Sugrañes, L. (1994). A simple radiometric correction model to improve automatic mapping of vegetation from multispectral satellite data. *Remote Sensing of Environment*, 48, 191-204.
- Purevdorj, T., Tateishi R., Ishiyama, T. and Honda, Y. (1998). Relationships between percent vegetation cover and vegetation indices. *International Journal of Remote Sensing*, 19(18), 3519-3535.
- Qi J., Huete, A. R., Moran, M. S., Chehbouni, A. & Jackson, R. D. (1993). Interpretation of vegetation indices derived from multi-temporal SPOT images. *Remote Sensing of Environment*, 44, 89-110.
- Qi, J., Chehbouni, A., Huete, A.R., Kerr, Y.H. and Sorooshian, S. (1994a). A modified soil adjusted vegetation index. *Remote Sens. Environ.* 48, 119-126.
- Qi, J., Kerr, Y. H. & Chehbouni, A. (1994b). External Factor Consideration in Vegetation Index Development. *Proceedings of Physical Measurements and Signatures in Remote Sensing*, ISPRS, 723-730.
- Razafimpanilo, H., Frouin, R., Iacobellis, S.F., & Somerville, R.C. (1995). Methodology for estimating burned area from AVHRR reflectance data. *Remote Sensing of Environment*, 54, 273-289.
- Retzlaff, R. (2000). Landscape analysis and fire hazard (A7). Final report of the LUCIFER project: Land use change interactions with fire in Mediterranean landscapes. Co-ordinated by J.M. Moreno. Universidad de Castilla la Mancha. Toledo. Spain.
- Richards, J.A. (1994). *Remote Sensing Digital Image Analysis: An Introduction*. Springer-Verlag. Berlin.
- Robinson, J.M. (1991). Fire from the space: global evaluation using infrared remote sensing. *International Journal of Remote Sensing*, 12, 3-24.
- Roberts, D.A., Smith M.O., & Adams J.B. (1993). Green vegetation, non-photosynthetic vegetation and soils in AVIRIS data. *Remote Sensing Environment*, 44, 255-269.
- Roberts, D.A., Batista, G.T., Pereira, J.L.G., Waller, E.K. & Nelson, B.W. (1998). Change identification using multitemporal spectral mixture analysis: applications in eastern Amazonia. In Lunetta & Elvidge (Ed) *Remote Sensing Change Detection. Environmental monitoring, methods and applications* (Pages 137-161). Ann Arbor Press, Chelsea, Michigan.

- Roberts et al., in press: Roberts, D.A., Numata, I., Holmes, K.W., Batista, G., Krug, T., Monteiro, A., Powell, B., and Chadwick, O. (2002). Large area mapping of land-cover change in Rondônia using multitemporal spectral mixture analysis and decision tree classifiers, *J. Geophys. Res. Atm.*, in press.
- Rodríguez-Silva, F., Navarro-Cerrillo, R., Navarro-Mezquita, C., & Gonzales-Dugo, M. (1997). Evaluation of Forest Fire Damage with Landsat-TM images and ancillary information. In E. Chuvieco (ed) *A review of remote sensing methods for the study of large wildland fires* (Pages 185-192), Publ. Universidad Alcalá, Alcalá de Henares, Spain.
- Rogan, J., Franklin, J., & D.A. Roberts. (2002). A comparison of methods for monitoring multitemporal vegetation change using Thematic Mapper imagery. *Remote Sensing of Environment*, 80, 142-156.
- Rouse, J.W., Hass, R.H., Schell, J.A., & Deering D.W. (1973). Monitoring Vegetation Systems in the Great Plains with ERTS-1. In *Proceedings of the Third Earth Resource Technology Satellite Symposium*, 1, 48-62.
- Ryherd, S & Woodcock, C. (1996). Combining spectral and texture data in the segmentation of remotely sensed images. *Photogrammetric Engineering and Remote Sensing*, 62, 181-194.
- Sabol, D.E., Adams, J.B., & Smith, M.O. (1992). Quantitative sub-pixel spectral detection of targets in multispectral images, *Journal of Geophysical Research*, 97, 2659-2672.
- Salvador, R., & Pons, X. (1996). Analysis of the discrimination of burnt sites temporal evolution in a Mediterranean area. *EARSel Advances in Remote Sensing*, 4, 159-169.
- Smith, M.O., & Adams, J.B. (1985). Strategy for analyzing mixed pixels in remotely sensed imagery. In *Proceedings of the NASA/JPL Aircraft SAR Workshop* (pages 47-48). JPL pub., Pasadena.
- Smits, P.C., Dellepiane, S.G., & Schowengerdt R.A. (1999). Quality assessment of image classification algorithms for land cover mapping: a review and a proposal for a cost-based approach. *International Journal of Remote Sensing*, 20, 1461-1487.
- Stehman, S.V. (1996). Estimating the Kappa-Coefficient and Its Variance Under Stratified Random Sampling: *Photogrammetric Engineering & Remote Sensing*, 62, 401-407.
- Soares, J.V., Rennó, C.D., Formaggio, A.R., Yanesse, C., and Frey, A.C. 1997. An investigation of the selection of texture features for crop discrimination using SAR imagery. *Remote Sensing of Environment* 59:234-247.
- Tanaka, S., Kimura, H., & Suga, Y. (1983). Preparation of a 1:125000 Landsat map for assessment of the burnt area on Etajima Island. *International Journal of Remote Sensing*, 4, 17-31.
- Waller, E.K. (1999). A comparison of Landsat multispectral scanner imagery and aerial photography for identifying land cover change in coastal southern California. Master's Thesis. UCSB, Santa Barbara.
- Wilson, J.D. (1992). A comparison of procedures for classifying remotely-sensed data using simulated data sets incorporating autocorrelations between spectral responses. *International Journal of Remote Sensing*, 13: 2701-2725.
- Xia, L. (1994). A two axis adjusted vegetation index (TWI). *International Journal of Remote Sensing*, 15:1447-1458.

WEBSites

WWW1: Climatic Atlas of Catalonia web. <http://www.uab.es/atles-climatic>

WWW2: Indian Space Research Organization. <http://www.isro.org/>